Journal of Power Sources 208 (2012) 197–202

Contents lists available at SciVerse ScienceDirect

Journal of Power Sources

journal homepage: www.elsevier.com/locate/jpowsour

The surface treatment of Ti meshes for use in large-area flexible dye-sensitized solar cells

Yaoming Xiao, Jihuai Wu*, Gentian Yue, Jianming Lin, Miaoliang Huang, Leqing Fan, Zhang Lan

Engineering Research Center of Environment-Friendly Functional Materials, Ministry of Education, Institute of Materials Physical Chemistry, Huaqiao University, Quanzhou 362021, China

ARTICLE INFO

Article history:
Received 3 October 2011
Received in revised form 27 January 2012
Accepted 6 February 2012
Available online 23 February 2012

Keywords:
Platinum counter electrode
Ti mesh
NaOH hydrothermal treatment
HF post-treatment
Large area
Flexible dye-sensitized solar cell

ABSTRACT

We report that NaOH hydrothermal treatment and HF post-treatment of the titanium mesh for the Pt/Ti counter electrode improved the efficiency of dye-sensitized solar cells. High performance platinum nanoparticles have been sprayed onto Ti meshes to form counter electrodes for use in large-area flexible DSSCs using a vacuum thermal decomposition method at low temperature (120 °C). The obtained Pt/Ti counter electrode shows low charge-transfer resistance (57.52 Ω cm^2 with active area of 80 cm^2) and high electrocatalytic activity for the I_3^-/I^- redox reaction. The photovoltaic properties and resistances of Pt/Ti counter electrodes with different HF post-treatment times of the NaOH treated Ti meshes have been investigated. The efficiency of the large-area (80 cm^2) flexible DSSC reaches 6.17% under irradiation with a natural light intensity of 55 mW cm^{-2} measured outdoors.

1. Introduction

Since the original fabrication of a dye-sensitized solar cell (DSSC) in 1991 by O'Regan and Grätzel [1–4], the flexible DSSC has attracted wide researches due to its merits, such as light weight, good flexibility, impact-proof, lower cost [5–13], and the flexible DSSC has been seen as the 3rd generation photovoltaic cell using roll-to-roll processing as well as the polymer solar cell [14,15], which could be a promising solution for many impending energy and environmental problems. A flexible DSSC with light-to-electric energy conversion efficiency of 7.2% has been achieved [6]. The fabrication of a flexible DSSC is possible using substrates such as metal foils and polymers. On the one hand, the Pt counter electrode on the flexible substrate is usually prepared by sputtering [7,8], electrochemical deposition [6,10,11], chemical reduction [5,12], and vacuum thermal decomposition method [16]. A high electrocatalytic activity for the I_3^-/I^- redox reaction and low series resistance of the Pt counter electrode is very significant in improving the performance of the DSSC, especially from the perspectives of its large scale production [17–19]. On the other hand, to enlarge cell sizes, several processes were attempted [17–21]. Commercial solar cells like poly-crystalline Si solar cells have a current-collecting grid that was made by silver solder or conductive printing paste to reduce their high surface resistance. In case of DSSC, unacceptable corrosion (or dissolution) of these materials in the contacting I^-/I_3^- redox electrolyte and the charge recombination between metal grids and redox electrolytes are the critical issues to be overcome [18].

Ti foils and Ti meshes have superior corrosion resistance in the contacting I^-/I_3^- electrolyte, due to the passive oxide film of TiO_2 on them. Therefore they have been utilized to manufacture flexible DSSCs as anodes, due to their flexibility and relatively low sheet resistance compared to that of conducting glass substrate [6,9,13]. Besides, the acid treatment of the Ti substrate for the photo-anode could improve the efficiency of DSSCs [22]. However, relatively few reports have focused on the surface treatment of Ti meshes for the Pt counter electrode. In this paper, we report on the surface treatment of Ti meshes using NaOH hydrothermal treatment and HF post-treatment, and the fabrication of large-area flexible dye-sensitized solar cells based on TiO_2 anodes on Ti foils and Pt/Ti counter electrodes on Ti meshes, shown in Fig. 1.

2. Experimental details

2.1. Materials

$H_2PtCl_6{\cdot}6H_2O$, ethanol, isopropanol, *n*-butanol iodine, lithium iodide, tetrabutyl ammonium iodide, 4-tert-butyl-pyridine, acetonitrile, titanium tetrachloride, sodium hydroxide, hydrofluoric acid, and hydrochloric acid were purchased from the

* Corresponding author. Tel.: +86 595 22693899; fax: +86 595 22692229.
E-mail addresses: ymxiao2011@sohu.com (Y. Xiao), jhwu@hqu.edu.cn (J. Wu).

0378-7753/$ – see front matter © 2012 Elsevier B.V. All rights reserved.
doi:10.1016/j.jpowsour.2012.02.019

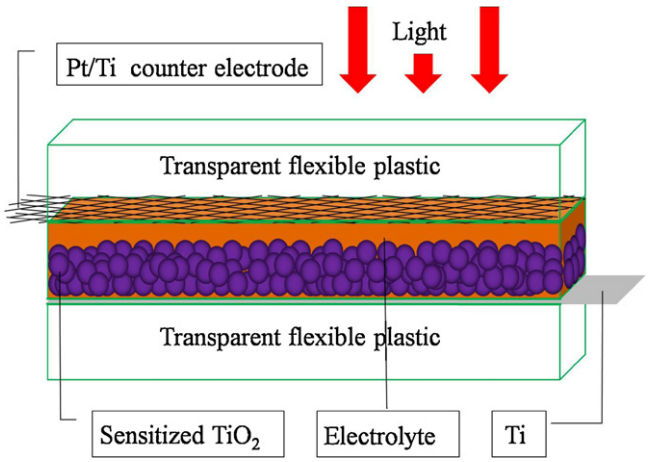

Fig. 1. Schematic diagram of large-area flexible dye-sensitized solar cells.

Shanghai Chemical Agent Ltd., China (Analysis purity grade). Sensitized-dye N719 [cis-di(thiocyanato)-*N*,*N*′-bis (2,2′-bipyridyl-4-carboxylic acid-4-tetrabutylammonium carboxylate) ruthenium (II)] was from Solaronix SA, Switzerland. The above agents were used without further purification.

2.2. Fabrication of flexible Pt/Ti counter electrodes

The Ti mesh (0.05 mm thickness, purchased from Anheng Wire Mesh Co., Ltd., China) was cleaned with mild detergent and rinsed in distilled water, then immersed in 0.20 mM HF solution for 5 min and rinsed in distilled water again. After cleaned, Ti meshes with rectangular dimension of 21 cm × 4.5 cm were placed into the Teflon-lined autoclave. The autoclaves were filled with 10 M NaOH solution (packing volume < 80%) and sealed into a stainless tank, individually. Then the systems were heated at 140 °C for 1 h. After that, the autoclaves were naturally cooled to room temperature, the obtained samples were washed with distilled water, with HCl aqueous solution (pH = 2) and then with distilled water for several times until the pH value of the samples equaled to 7. The products were sintered at 400 °C for 30 min in air to produce TiO_2 nanowires, then immersed in 0.20 mM HF solution for a post-treatment with different times and rinsed in distilled water again, thus the NaOH treatment Ti meshes were obtained. $H_2PtCl_6{\cdot}6H_2O$ was dissolved in isopropanol and *n*-butanol (volume ratio of 1:1) with concentration of 0.96% to prepare $H_2PtCl_6{\cdot}6H_2O$ solution and then sprayed on both sides of the NaOH treatment Ti meshes. Ti meshes were heated at 120 °C for 2 h in a vacuum drying oven (Suzhou Jiangdong Precision Instrument Co., Ltd., China) [16], the Pt thus was deposited on Ti meshes to form Pt/Ti counter electrodes with NaOH treatment and HF post-treatment. For comparison, the Pt/Ti counter electrode without NaOH treatment was also prepared, which was designated as Sample A. The Pt/Ti counter electrode with NaOH treatment, and then with HF post-treatment for 5 min was designated as Sample B, 10 min as Sample C, and 15 min as Sample D.

2.3. Preparation of flexible TiO_2/Ti anodes

The TiO_2 colloid (prepared according to our previous reports [16,23–25]) was coated on the Ti foil (0.03 mm thickness, purchased from Baoji Yunjie Metal Production Co., Ltd., China) using a doctor-scraping technique. Before the scraping, Ti foils with rectangular dimension of 21 cm × 4.5 cm were washed with mild detergent and rinsed in distilled water, then immersed in 0.20 mM HF solution for 5 min and rinsed in distilled water again. The thickness of the TiO_2 film was controlled by the thickness of the adhesive tape around the edge of the cleaned Ti foil [23–25]. After drying at room temperature, the TiO_2 thin films were sintered at 400 °C for 30 min in air to produce nanocrystalline TiO_2 films, the TiO_2 electrodes were immersed in a 0.05 M $TiCl_4$ solution at 70 °C for 30 min, and then washed three times with distilled water. The treated TiO_2 films were sintered at 400 °C for 20 min. When the TiO_2 electrodes were cooled to 80 °C, the obtained TiO_2/Ti electrodes were treated by ultraviolet–O_2 at room temperature for 30 min. The TiO_2 flexible film was immersed in a 2.50×10^{-4} M solution of dye N719 in absolute ethanol for 24 h. This allowed sufficient time for the TiO_2 film to absorb the dye adequately. Thus, a dye-sensitized TiO_2 flexible film electrode was obtained.

2.4. Assemblage of flexible DSSCs

The flexible DSSC with an active area of 20 cm × 4.0 cm was assembled by injection of a redox-active electrolyte into the aperture between the TiO_2 film electrode (anode) and the Pt/Ti counter electrode (as shown in Fig. 1). The two electrodes were clipped together with two transparent flexible plastics and a cyanoacrylate adhesive was used as a sealant to prevent the electrolyte solution from leaking. Epoxy resin was used to further seal the cell in order to measure the cell stability. The redox electrolyte consisted of 0.60 M tetrabutyl ammonium iodide, 0.10 M lithium iodide, 0.10 M iodine, and 0.50 M 4-tert-butyl-pyridine in acetonitrile.

2.5. Characterization

The surface features of flexible Pt/Ti counter electrodes were observed using a scanning electron microscope (SEM, Hitachi S-4800, Japan), an energy-dispersive X-ray spectrometer (EDX) attached to the SEM. The cyclic voltammetry (CV) profiles of the Pt/Ti counter electrode was measured in a three-electrode electrochemical cell with an Electrochemical Workstation (CHI660D, Shanghai Chenhua Device Company, China) using the Pt/Ti as the working electrode, a Pt-foil as counter electrode, and an Ag/AgCl as reference electrode dipped in an acetonitrile solution of 10 mM LiI, 1 mM I_2, and 0.1 M $LiClO_4$. The CV measurements were performed using CHI660D electrochemical measurement system (scan condition: 25 mV s^{-1}, 50 mV s^{-1}, 100 mV s^{-1}, 250 mV s^{-1}, and 500 mV s^{-1}). Electrochemical impedance spectroscopy (EIS) measurements of the large-area flexible DSSCs were carried out using a CHI660D electrochemical measurement system at a constant temperature of 20 °C, with an AC signal amplitude of 20 mV in the frequency range from 0.1 to 10^5 Hz at zero V DC bias, in the dark. The IPCE (incident monochromatic photon-to-current conversion efficiency) curves were measured with a Newport Monochromator (Power Meter Model 2936-C, Newport Corporation, USA).

2.6. Photoelectrochemical measurements

The photovoltaic performance test of the flexible DSSC was conducted by measuring the *I*–*V* character curves using a CHI660D electrochemical measurement system under irradiation with natural light intensity (measured by Radiometer FZ-A, Photoelectric Inst. of Beijing Normal Univ., China) of 55 mW cm^{-2} out of doors. The photovoltaic performance [i.e. fill factor (FF) and overall energy conversion efficiency (η)] of the DSSC was calculated using the following equations [26]:

$$\mathrm{FF} = \frac{V_{\max} \times \mathrm{I}_{\max}}{V_{\mathrm{oc}} \times I_{\mathrm{sc}}} \tag{1}$$

$$\eta\ (\%) = \frac{V_{\max} \times \mathrm{I}_{\max} \times 100}{P_{\mathrm{in}}} = \frac{V_{\mathrm{oc}} \times I_{\mathrm{sc}} \times \mathrm{FF} \times 100}{P_{\mathrm{in}}} \tag{2}$$

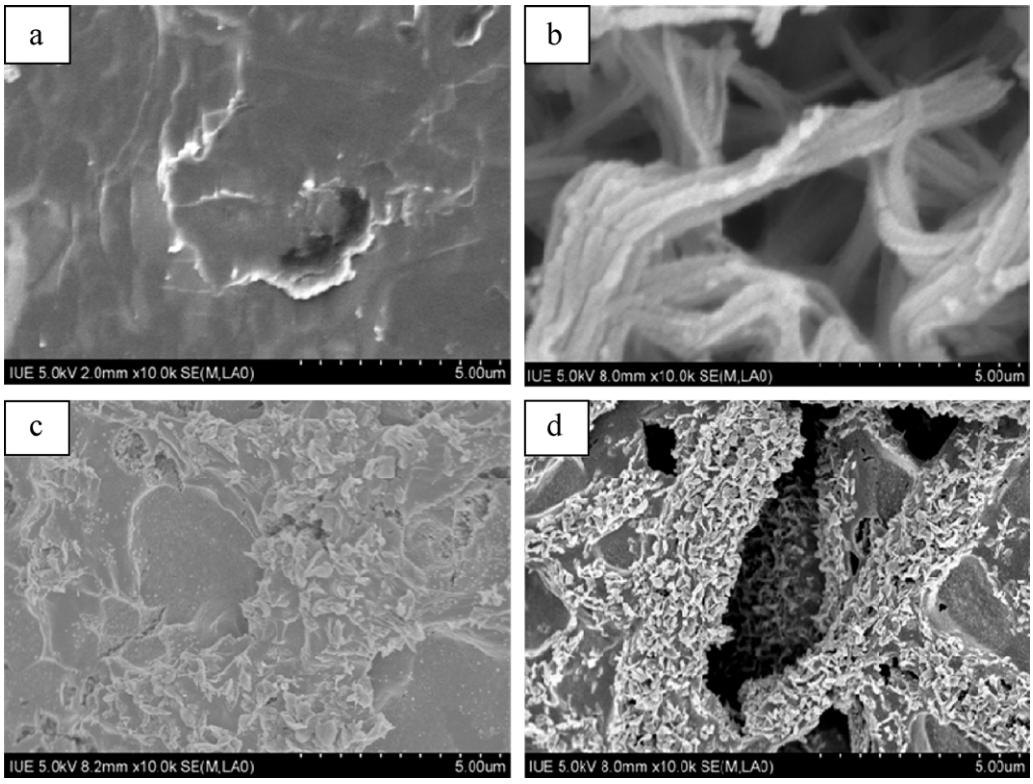

Fig. 2. SEM images of the cleaned Ti mesh (a), the NaOH treatment Ti mesh (b), and Pt/Ti counter electrodes based on the Sample A (c) and Sample B (d).

where I_{sc} is the short-circuit current (A), V_{oc} is the open-circuit voltage (V), P_{in} is the incident light power (W), and I_{max} (A) and V_{max} (V) are the current and voltage in the *I–V* curves, respectively, at the point of maximum power output.

3. Results and discussion

3.1. Morphology and compositions of Pt/Ti counter electrodes

Fig. 2(a) shows the SEM image of the Ti mesh cleaned in the 0.20 mM HF solution. It is obvious that the surface of the cleaned Ti mesh is roughened after immersed in the HF solution. As shown on the Fig. 2(b), TiO_2 nanowires were produced on the cleaned Ti mesh after a NaOH hydrothermal treatment, and this Ti mesh has a higher void space than the Ti mesh only cleaned in the HF solution. Fig. 2(c) and (d) shows the SEM images of Pt/Ti counter electrodes based on the Sample A and Sample B. It is obvious that Pt particles have been dispersed on the Ti mesh with a size diameter of about 200–400 nm. When H_2PtCl_6 was heated at 120 °C for 2 h in a vacuum environment, the reaction equations are listed as follows: $H_2PtCl_6{\cdot}6H_2O \leftrightarrow PtCl_4 + 2HCl + 6H_2O$; $PtCl_4 \leftrightarrow PtCl_2 + Cl_2$; $PtCl_2 \leftrightarrow Pt + Cl_2$. As we know, the three reversible reactions produce gaseous products, and the vacuum condition promotes the positive direction reaction, which results in complete decomposition of H_2PtCl_6 at low temperature in a vacuum drying oven [16]. As shown, the Pt/Ti counter electrode prepared with NaOH treatment and 10 min HF post-treatment has three-dimensional space to hold more Pt particles than the Pt/Ti counter electrode without NaOH treatment, leading to the former has higher electrocatalytic activity for the I_3^-/I^- redox reaction than the latter.

3.2. Electrochemical properties of Pt/Ti counter electrodes

Fig. 3 shows cyclic voltammograms for Pt/Ti counter electrodes based on the Sample A and Sample B. The two kinds of counter electrodes show two pairs of oxidation and reduction peaks, which suggests the obtained Pt/Ti counter electrodes have comparatively similar electrocatalytic activity for the I_3^-/I^- redox process. The oxidation and reduction pair (peaks B_{ox} and B_{red}) on the right is attributed to the redox reaction of $I_3^- + 2e^- \rightarrow 3I^-$, which directly affects the DSSC performance; the redox pair (peaks A_{ox} and A_{red}) on the left results from the reaction of $3I_2 + 2e^- \rightarrow 2I_3^-$, which has little effect on the DSSC performance [27,28]. The Pt/Ti counter electrode with NaOH treatment and 10 min HF post-treatment shows larger oxidation and reduction current density than the Pt/Ti electrode without NaOH treatment, suggesting a fast rate of triiodide reduction, which is consistent with the Fig. 2(c) and (d).

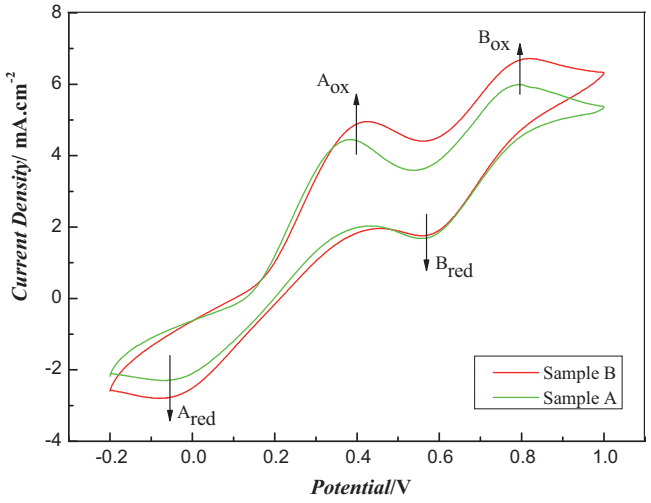

Fig. 3. Cyclic voltammograms for Pt/Ti electrodes based on the Sample A and Sample B at the scan rate of 100 mV s^{-1}.

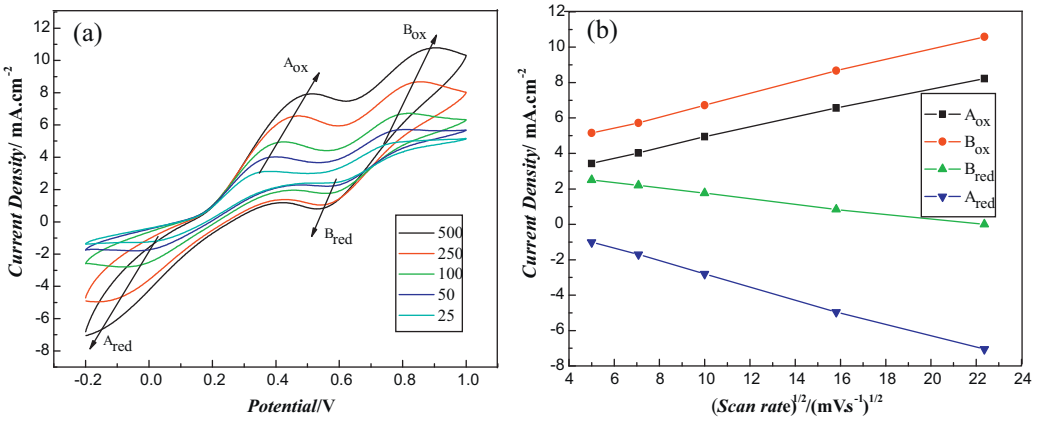

Fig. 4. (a) Cyclic voltammograms for Pt/Ti electrode with different scan rates (from inner to outer: 25, 50, 100, 250 mV s^{-1}, and 500 mV s^{-1}, respectively), (b) relationship between all the redox peak currents and scan rates.

Fig. 4a shows CVs of the I_3^-/I^- system on the Pt/Ti counter electrode (prepared with NaOH treatment and 10 min HF post-treatment) with different scan rates. This figure shows that the peak current densities change with the scan rate. The cathodic peaks gradually and regularly shift negatively, and the corresponding anodic peaks shift positively with increasing scan rate. Fig. 4b illustrates the relationship between the cathodic and anodic peak currents and the square root of the scan rate. The linear relationship at various scan rates indicates that this redox reaction is diffusion limited at the Pt/Ti counter electrode, which may be a result of transport of iodide species off of the Pt/Ti counter electrode surface [29,30]. This phenomenon shows that the adsorption of iodide species is little affected by the redox reaction on the Pt/Ti counter electrode surface, suggesting no specific interaction between the I_3^-/I^- redox couple and the Pt/Ti counter electrode [29].

Fig. 5 shows 400 successive CV cycles of the Pt/Ti counter electrode based on the Sample B. On consecutive scans, the peak positions and current densities hardly change. This indicates that the Pt particles are tightly bound to the Ti mesh surface [31].

3.3. Influence of the NaOH treatment and HF post-treatment on the photovoltaic properties

Fig. 6 shows the structure diagram of the Ti mesh and the computational formula of light transmittance of the Ti mesh. Where TB is the diagonal line breadth, TL is the diagonal line length of the Ti mesh and W is the width of the Ti mesh infarction. In this paper, we choose the Ti mesh, whose TB is 1.5 mm, TL is 2.0 mm and W is 0.05 mm, therefore the light transmittance is 92.31% calculated using the computational formula.

Fig. 7 shows the *I–V* curves of flexible DSSCs (active area of 80 cm^2) based on the Sample A and Sample B under natural light intensity of 55 mW cm^{-2} and in the dark, respectively. The V_{oc} depends greatly on recombination behavior. *I–V* measurements under dark condition show clearly that recombination of the Sample B cell is smaller than that of the Sample A cell, which indicates that the internal consumption of current is lower, leading to the higher open-circuit voltage. Therefore, the V_{oc} of the DSSC based on the Sample B is higher than that of the Sample A. The I_{sc} values are comparatively low, due to the passive oxide film of TiO_2 on Ti substrates, thereby, Ti foils and Ti meshes have superior corrosion resistance in the contacting I^-/I_3^- electrolyte.

Fig. 8 shows the IPCE curves of the flexible DSSCs based on the Sample A and Sample B. It is noticeable that the IPCE curve for the flexible DSSC using the Pt/Ti counter electrode with NaOH treatment and 10 min HF post-treatment from 400 nm to 680 nm is higher than that for the Pt counter electrode without NaOH treatment, resulting in a difference in I_{sc}. The I_{sc} value of the Pt/Ti counter electrode based on the Sample B shows higher than that of the

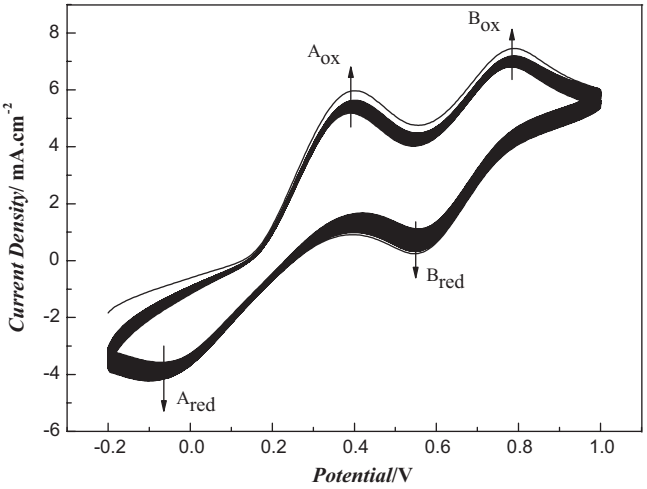

Fig. 5. Consecutive 400 cyclic voltammograms of I_2/I^- system for the Pt/Ti electrode at a scan rate of 100 mV s^{-1}.

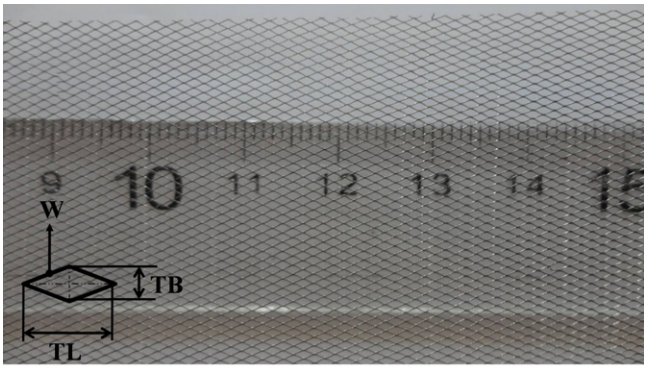

$$\text{Light transmittance}(\%) = \frac{\frac{1}{2}TB \times TL}{\frac{1}{2}TB \times TL + 4 \times (\frac{1}{2}W) \times \sqrt{(\frac{1}{2}TB)^2 + (\frac{1}{2}TL)^2}} \times 100\%$$

Fig. 6. Structure diagram and the computational formula of light transmittance of the Ti mesh.

Table 1
The photovoltaic performance of DSSCs with different HF post-treatment times.

HF post-treatment time (min)	Sun (mW cm^{-2})	I_{sc} (A)	J_{sc} (mA cm^{-2})	V_{oc} (V)	FF	η (%)	P_{max}[a] (W)
5	55	0.508	6.35	0.711	0.698	5.73	0.252
10	55	0.527	6.59	0.718	0.717	6.17	0.271
15	55	0.511	6.39	0.714	0.719	5.96	0.262

[a] $P_{max} = I_{sc} \times V_{oc} \times FF$.

Sample A. This is due to the effect of scattering and electrocatalytic activity of the counter electrode. On the one hand, the proper amount of Pt particles can enhance the scattering effect to increase the absorption and utilization of light [32]. On the other hand, the Pt/Ti counter electrode prepared with NaOH treatment and 10 min HF post-treatment has three-dimensional space to hold more Pt particles than the Pt/Ti counter electrode without NaOH treatment, increasing the rate of the I_3^-/I^- redox reaction at the Pt counter electrode [29,33], thereby enhancing the electrocatalytic activity of the counter electrode. Therefore, the η and P_{max} values of the Pt/Ti counter electrode based on the Sample B show higher than that of the Sample A.

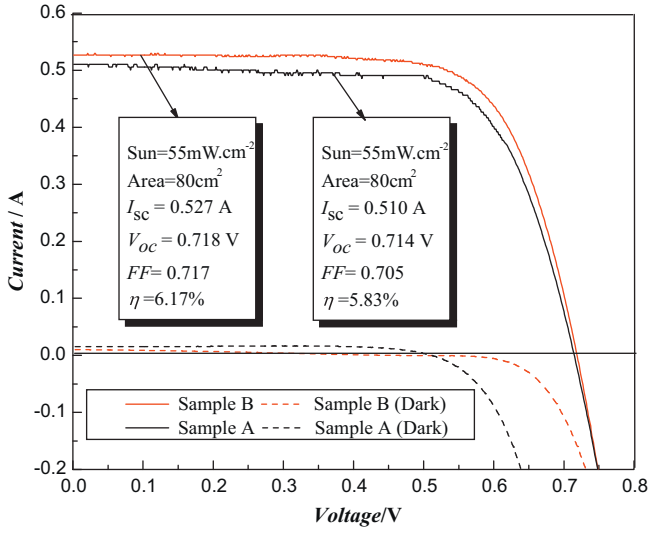

Fig. 7. *I–V* curves of flexible DSSCs based on the Sample A and Sample B.

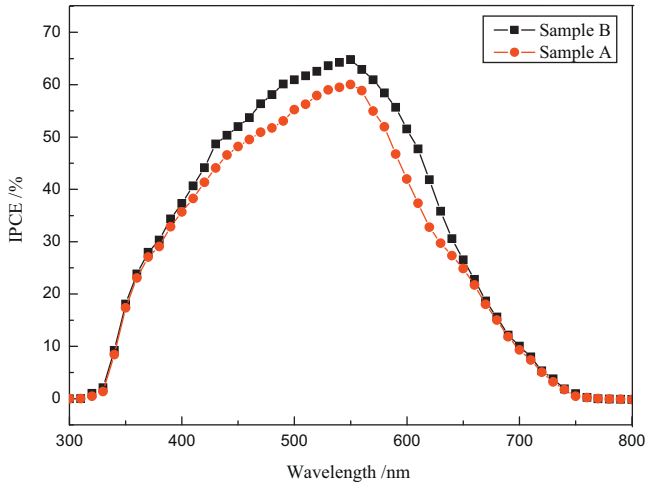

Fig. 8. IPCE spectra of the flexible DSSCs based on the Sample A and Sample B.

3.4. Influence of the HF post- treatment time on the photovoltaic properties

Electrochemical impedance spectroscopy (EIS) was measured with large-area (active area of 80 cm^2) flexible DSSCs based on Pt/Ti counter electrodes with different HF post-treatment times (shown in Fig. 9), where R_S represents mainly the series resistance of the Ti substrate, and R_{CT} is the charge-transfer resistance at the interface between electrolyte and the electrode for the I_3^-/I^- redox reaction [28,34–36], and the results of the R_S and R_{CT} are shown in the table accompanying the Fig. 9. As shown in Fig. 9, the R_{CT} reduces with the increase of the HF post-treatment time, this is due to that the thickness of TiO_2 nanowires film on the Ti mesh was cut down by the HF solution. Therefore, the Pt/Ti counter electrode based on the less time has a lower electrical conductivity, this is disadvantageous to electron transport [37–39].

The photovoltaic performances of DSSCs (active area of 80 cm^2) based on different HF post-treatment times are shown in the Table 1. It can be found that the I_{sc} value increases firstly and then decreases with the increase of the HF post-treatment time, this trend is due to the R_{CT} and electrocatalytic activity of the counter electrode. In other words, the R_{CT} reduces with the increase of the HF post-treatment time, which is advantageous to electron transport [37–39], leading to higher I_{sc}; however, the void space of the Ti mesh reduces, which is disadvantageous to hold Pt particles, resulting in lower electrocatalytic activity and I_{sc}. The proper three-dimensional space could hold a large amount of Pt particles, which

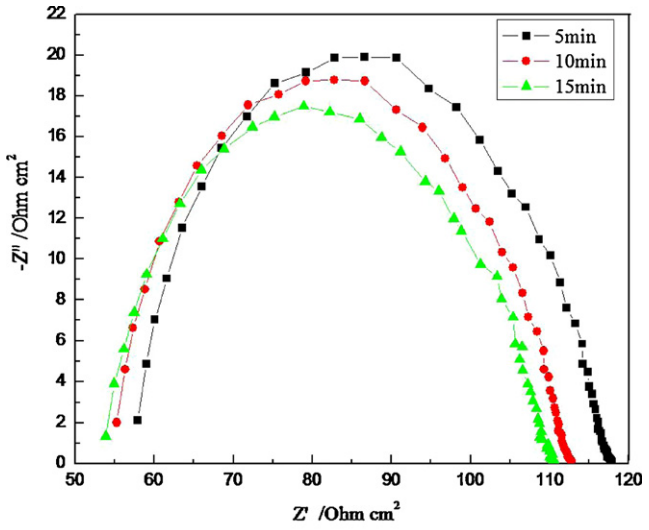

Time (min)	R_S (Ω·cm^2)	R_{CT} (Ω·cm^2)
5	57.92±0.05	59.92±0.05
10	55.27±0.04	57.52±0.03
15	53.85±0.02	56.42±0.04

Fig. 9. EIS (measured in the dark) of flexible DSSCs with different HF post-treatment times.

could enhance the electrocatalytic activity, resulting in higher I_{sc}. Compared the cells with increasing the HF post-treatment time, the change trend of the V_{oc} is in accordance with the I_{sc}. However, the fill factor (FF) values increase with the increase of the HF post-treatment time, this is because of the values of the R_{CT} reduces with the increase of the HF post-treatment time [17,18]. Therefore, the η and P_{max} values of the DSSC increase firstly and then decreases with the increase of the HF post-treatment time.

4. Conclusion

In summary, the titanium mesh was utilized to form the large-area flexible Pt/Ti counter electrode using the vacuum thermal decomposition method at low temperature (120 °C). Before the vacuum thermal decomposition, the Ti mesh was treated using the NaOH hydrothermal treatment and HF post-treatment for the Pt/Ti counter electrode improved the efficiency of DSSCs. Based on the optimum HF post-treatment time of 10 min, the obtained Pt/Ti counter electrode shows low charge-transfer resistance of $57.52 \pm 0.03\,\Omega\,cm^2$ with area of $80\,cm^2$, and has high electrocatalytic activity for the I_3^-/I^- redox reaction. The light-to-electric energy conversion efficiency of the large-area ($80\,cm^2$) flexible DSSC reaches 6.17% under irradiation with a natural light intensity of $55\,mW\,cm^{-2}$ measured out of doors. Compared with other methods and materials to prepare Pt counter electrodes, the NaOH hydrothermal treatment and the HF post-treatment on the Ti mesh are suitable and low cost for the large scale preparation of Pt counter electrodes and flexible DSSCs.

Acknowledgments

The authors thank for the joint support by the National High Technology Research and Development Program of China (No. 2009AA03Z217) and the National Natural Science Foundation of China (No. 90922028, 51002053).

References

[1] B.O' Regan, M. Grätzel, Nature 353 (1991) 737–740.
[2] M. Grätzel, Inorg. Chem. 44 (2005) 6841–6851.
[3] M. Grätzel, Acc. Chem. Res. 42 (2009) 1788–1798.
[4] M. Grätzel, Nature 414 (2001) 338–344.
[5] M.G. Kang, N.G. Park, K.S. Ryu, S.H. Changa, K.J. Kim, Sol. Energy Mater. Sol. Cells 90 (2006) 574–581.
[6] S. Ito, N.C. Ha, G. Rothenberger, P. Liska, P. Comte, S.M. Zakeeruddin, P. Péchy, M.K. Nazeeruddin, M. Grätzel, Chem. Commun. 38 (2006) 4004–4006.
[7] M. Ikegami, K. Miyoshi, T. Miyasak, Appl. Phys. Lett. 90 (2007) 153122.
[8] L.Y. Lin, C.P. Lee, R. Vittal, K.C. Ho, J. Power Sources 195 (2010) 4344–4349.
[9] Y.M. Xiao, J.H. Wu, G.T. Yue, G.X. Xie, J.M. Lin, M.L. Huang, Electrochim. Acta 55 (2010) 4573–4578.
[10] X. Yin, Z.S. Xue, B. Liu, J. Power Sources 196 (2011) 2422–2426.
[11] W.H. Chiu, K.M. Lee, W.F. Hsieh, J. Power Sources 196 (2011) 3683–3687.
[12] J.H. Park, Y. Jun, H.G. Yun, S.Y. Lee, M.G. Kang, J. Electrochem. Soc. 155 (2008) F145–F149.
[13] V. Vijayakumar, A.D. Pasquier, D.P. Birnie III, Sol. Energy Mater. Sol. Cells 95 (2011) 2120–2125.
[14] F.C. Krebs, T. Tromholt, M. Jorgensen, Nanoscale 2 (2010) 873–886.
[15] F.C. Krebs, T.D. Nielsen, J. Fyenbo, M. Wadstrom, M.S. Pedersen, Energy Environ. Sci. 3 (2010) 512–525.
[16] Y.M. Xiao, J.H. Wu, G.T. Yue, J.M. Lin, M.L. Huang, Z. Lan, Electrochim. Acta 56 (2011) 8545–8550.
[17] W.J. Lee, E. Ramasamy, D.Y. Lee, J.S. Song, J. Photochem. Photobiol. A 183 (2006) 133–137.
[18] E. Ramasamy, W.J. Lee, D.Y. Lee, J.S. Song, J. Power Sources 165 (2007) 446–449.
[19] D.H. Yeon, K.K. Kim, N.G. Park, Y.S. Cho, J. Am. Ceram. Soc. 93 (2010) 1554–1556.
[20] G.R.A. Kumara, S. Kaneko, A. Konno, M. Okuya, K. Murakami, B. Onwona-agyeman, K. Tennakone, Prog. Photovolt.: Res. Appl. 14 (2006) 643–651.
[21] S. Noda, K. Nagano, E. Inoue, T. Egi, T. Nakashima, N. Imawaka, M. Kanayama, S. Iwata, K. Toshima, K. Nakada, K. Yoshino, Synth. Met. 159 (2009) 2355–2357.
[22] G. Yun, B.S. Bae, M.G. Kang, Adv. Energy Mater. 1 (2011) 337–342.
[23] J.H. Wu, Z. Lan, J.M. Lin, M.L. Huang, S.C. Hao, T. Sato, S. Yin, Adv. Mater. 19 (2007) 4006–4011.
[24] J.H. Wu, S.C. Hao, Z. Lan, J.M. Lin, M.L. Huang, Y.F. Huang, P.J. Li, S. Yin, T. Sato, J. Am. Chem. Soc. 130 (2008) 11568–11569.
[25] Z. Lan, J.H. Wu, S.C. Hao, J.M. Lin, M.L. Huang, Y.F. Huang, Energy Environ. Sci. 2 (2009) 524–528.
[26] M. Grätzel, Prog. Photovolt.: Res. Appl. 8 (2000) 171–185.
[27] Z. Huang, X.Z. Liu, K.X. Li, D.M. Li, Y.H. Luo, H. Li, W.B. Song, L.Q. Chen, Q.B. Meng, Electrochem. Commun. 9 (2007) 596–598.
[28] X. Mei, S. Cho, B. Fan, J.Y. Ouyang, Nanotechnology 21 (2010) 395202.
[29] Y. Saito, W. Kubo, T. Kitamura, Y. Wada, S. Yanagida, J. Photochem. Photobiol. A 164 (2004) 153–157.
[30] S. Biallozor, A. Kupniewska, Electrochem. Commun. 2 (2000) 480–486.
[31] H. Guo, Y. Li, L. Fan, X. Wu, M. Guo, Electrochim. Acta 51 (2006) 6230–6237.
[32] H. Han, S. Lee, H. Shin, H.S. Jung, Adv. Energy Mater. 1 (2011) 546–550.
[33] K. Imoto, K. Takahashi, T. Yamaguchi, T. Komura, J. Nakamura, K. Murata, Sol. Energy Mater. Sol. Cells 79 (2003) 459–469.
[34] G. Li, F. Wang, Q. Jiang, X. Gao, P. Shen, Angew. Chem. Int. Ed. 49 (2010) 3653–3656.
[35] F. Fabregat-Santiago, J. Bisquert, G. Garcia-Belmonte, G. Boschloo, A. Hagfeldt, Sol. Energy Mater. Sol. Cells 87 (2005) 117–131.
[36] M. Adachi, M. Sakamoto, J. Jiu, Y. Ogata, S. Isoda, J. Phys. Chem. B 110 (2006) 13872–13880.
[37] A. Fujiwara, Y. Matsuoka, Y. Matsuoka, H. Suematsu, N. Ogawa, K. Miyano, H. Kataura, Y. Maniwa, S. Suzuki, Y. Achiba, Carbon 42 (2004) 919–922.
[38] S. Moriyama, K. Toratani, D. Tsuya, M. Suzuki, Y. Aoyagi, K. Ishibashi, Physica E 24 (2004) 46–49.
[39] G. Mor, K. Shankar, M. Paulose, O. Varghese, C. Grimes, Nano Lett. 6 (2006) 215–218.